

# The LMR-SSIGN-MAPS model predicts disease-free survival in patients with localized clear cell renal cell carcinoma

Hongzhuang Wen<sup>1</sup>, Yong Zhang<sup>2</sup>, Zhan Yang<sup>1</sup>, Zhao Zhai<sup>2</sup>, Zhenwei Han<sup>1</sup>, Hu Wang<sup>1</sup>, Mingshuai Wang<sup>1</sup>, Hongzhe Shi<sup>2</sup>, Xi Chen<sup>2</sup>, Wasilijiang Wahafu<sup>2</sup>, Kaopeng Guan<sup>2</sup>, Xiaolu Wang<sup>1</sup>

<sup>1</sup>Department of Urology, The Second Hospital of Hebei Medical University, Shijiazhuang, China

<sup>2</sup>National Cancer Centre, National Clinical Research Centre for Cancer, Cancer Hospital, Chinese Academy of Medical Sciences and Peking Union Medical College, Beijing, China

Videosurgery Miniinv 2023; 18 (2): 313–327

DOI: <https://doi.org/10.5114/wiitm.2022.123455>

## Abstract

**Introduction:** Prediction models are increasingly being used to predict outcomes after surgery, and such a model would be a precious tool for patients with clear cell renal cell carcinoma (ccRCC) after surgery.

**Aim:** To develop a comprehensive model for predicting disease-free survival (DFS) in patients with localized ccRCC.

**Material and methods:** In a retrospective analysis of 612 patients, least absolute shrinkage and selection operator (LASSO) Cox regression analysis was performed to identify significant predictors, and then risk factors were used to construct a prognostic model. Harrell's concordance index (C-index) was used to assess the accuracy of the model.

**Results:** The lymphocyte-to-monocyte ratio (LMR), Mayo Clinic stage, size, grade, necrosis score (SSIGN), and Mayo adhesive probability score (MAPS) were the significant risk factors screened by LASSO Cox regression and reconfirmed by multivariate Cox regression analysis in 44 variables. Then a model was constructed by combining the LMR, SSIGN, and MAPS. The C-index of the LMR-SSIGN-MAPS model was greater than the SSIGN score alone. Kaplan-Meier survival analysis demonstrated a significant association between higher LMR-SSIGN-MAPS score and poorer DFS.

**Conclusions:** The LMR-SSIGN-MAPS model, which consists of preoperative inflammation biomarkers, a perinephric adipose tissue image-based scoring system, and pathological features, showed the strengths of easy-to-use and high predictability and might also be used as a promising prognosis model in predicting DFS for patients with localized ccRCC.

**Key words:** biomarkers, renal cell carcinoma, disease-free survival, prognosis, regression analysis.

## Introduction

The incidence of renal cell carcinoma (RCC) is on the rise yearly worldwide. According to global cancer data from 2020, kidney cancer ranked 14<sup>th</sup> in terms of incidence rate (2.2%) and 15<sup>th</sup> in terms of mortality rate (1.8%) [1]. Although nephrectomy can be a curative procedure, approximately 30% of patients with localized clear cell RCC (ccRCC) eventually developed to a metastatic stage, which requires

systemic therapy and is associated with high mortality [2].

The inflammatory responses are critical in tumour initiation, progression, invasion, and metastasis development [3]. Moreover, systemic inflammatory markers including neutrophils, lymphocytes, monocytes, and the lymphocyte-to-monocyte ratio (LMR) have shown prognostic value in RCC [4, 5]. During renal carcinogenesis, the renal cancer cells can penetrate the renal capsule and can infiltrate

### Address for correspondence

Dr Xiaolu Wang, Department of Urology, The Second Hospital of Hebei Medical University, Shijiazhuang, China, e-mail: wxlurology@163.com

the perirenal adipose tissue (PRAT) [6], a process associated with a poor prognosis [7]. The thermogenic activity of perirenal adipocytes promotes the growth, invasion, and metastasis of the renal cancer cells and reduces their antitumour efficacy through the interaction of the renal cancer cells with the adjacent PRAT [8]. The Mayo adhesive probability score (MAPS) is an accurate imaging scoring system in predicting PRAT adhesion, which was first proposed in robotic-assisted partial nephrectomy [9]. Higher MAPS were associated with poor progression-free survival of patients with localized RCC treated with surgery [10]. The Mayo Clinic stage, size, grade, and necrosis (SSIGN) score comprise a dependable, accessible model with a prognostic value on the basis of readily obtained variables from the clinician and pathologist [11].

The predictive models combining information from multiple factors are widely accepted for their value in counselling patients and determining the necessity of an adjuvant therapy in the genitourinary oncology [11]. However, the joint utilization of preoperative cancer-related inflammation biomarkers, PRAT image-based scoring system, and tumour characteristics for prognosis of patients with localized ccRCC has not been covered.

## Aim

This study was designed to assess the clinical implication of a newly proposed prognostic model for predicting DFS in patients with localized ccRCC. This model was a joint utilization of the LMR, SSIGN, and MAPS, termed as the LMR-SSIGN-MAPS.

## Material and methods

### Population

From January 2010 to December 2015, a total of 1834 patients with localized ccRCC, who underwent radical or partial nephrectomy at the Department of Urology of the Cancer Hospital Chinese Academy of Medical Sciences, were reviewed with retrospection.

The enrolment standards for this study were as follows: (1) no other solid tumours prior to surgery; (2) no history of using statins for hyperlipidaemia; (3) no thyroid disease, no liver or kidney dysfunction; (4) no bilateral or multiple ccRCC, no previous kidney surgery or kidney injury; (5) no signs of extrarenal metastases and preoperative adjuvant ther-

apy; (6) definitive pathological diagnosis and complete resection of tumour with negative margins; (7) complete preoperative medical information or follow-up data; and (8) available preoperative MAPS measurements with computerized tomography (CT) or magnetic resonance imaging (MRI) scan.

Finally, 612 patients were integrated into this study. The study protocol was authorized by the Ethics Committee of the Cancer Hospital Chinese Academy of Medical Sciences. Furthermore, all patients supplied informed consent.

### Data collection

Clinical information, consisting of general demographic variables, preoperative peripheral haematological indicators, pathological characteristics, and MAPS, were collected (Table I). Tumours were routinely fixed in 10% formalin, and paraffin-embedded sections were stained with haematoxylin and eosin (H&E). The pathological features were assessed by 2 senior pathologists on the basis of the Fuhrman grading system and the 2010 American Joint Commission on tumour-node-metastasis staging [12, 13]. Additionally, some indicators derived from preoperative peripheral blood that have been reported to be significant for the prognosis of renal cell carcinoma were collected. Castelli risk index-I (CRI-I) was defined as the ratio of total cholesterol (TC) to high-density lipoprotein cholesterol (HDL-C), while Castelli risk index-II (CRI-II) was defined as the ratio of low-density lipoprotein cholesterol (LDL-C) to HDL-C [14]. The prognostic nutritional index (PNI) was defined as albumin + 5 × lymphocyte [15]. The preoperative controlling nutritional status (CONUT) score was calculated on the basis of the serum albumin level, total lymphocyte count, and total cholesterol level [16]. The systemic inflammation score (SIS) was calculated on the basis of preoperative serum albumin and LMR [17].

The MAPS was computed by 2 measurements as follows: the thickness of the posterior renal fat and the extent of the perirenal fat stranding around the renal tumour at the level of the renal vein on CT scan or T1 MRI scan (Photo 1). The thickness of the posterior renal fat was calculated as the distance between the posterior renal capsule and the body in centimetres (< 1 cm = 0 points; 1.0–1.9 = 1 points; ≥ 2.0 cm = 2 points). A perirenal fat stranding extent score was acquired at one level (no stranding = 0

**Table I.** Variables in the analysis (*n* = 44)

Variables	
Preoperative peripheral haematological indicators ( <i>n</i> = 24)	White blood cell, neutrophil, lymphocytes, monocytes, Red blood cell, haemoglobin, platelet, total proteins Albumin, globulin, albumin/globulin(A/G) Total cholesterol, triglyceride, low-density lipoprotein cholesterol, high-density lipoprotein cholesterol, Castelli risk index-I (CRI-I), Castelli risk index-II (CRI-II) Neutrophil-to-lymphocyte ratio (NLR) Monocyte-to-lymphocyte ratio (MLR) Platelet-to-lymphocyte ratio (PLR)Lymphocyte-to-monocyte ratio (LMR) Prognostic nutritional index (PNI) Controlling nutritional status (CONUT) score Systemic inflammation score (SIS)
General demographic variables ( <i>n</i> = 12)	Age, sex, diabetes status, hypertension Hyperlipidaemia, coronary heart disease, smoking Drinking, body mass index (BMI), laterality (left/right) Operative extent (partial nephrectomy/radial nephrectomy), nephrectomy (laparoscopic/open surgery)
Pathological characteristics ( <i>n</i> = 7)	PT1, PT2, PT3, Fuhrman grade, tumour size, necrosis The Mayo Clinic stage, size, grade, and necrosis (SSIGN) score
Image-based scoring system ( <i>n</i> =1)	Mayo adhesive probability score (MAPS)

points, mild stranding = 2 points, severe stranding = 3 points). The total score (0–5 points) was obtained by adding the 2 scores together [9].

The SSIGN score was calculated based on tumour stage, size, grade, and necrosis as follows. (i) T-stage: 0 points for pT1 and pT4, 1 point for pT2 and 2 points for pT3; (ii) N-stage: 0 points for pNx and pN0, 2 points for pN1 and pN2; (iii) M-stage: 0 points for pM0 and 4 points for pM1; (iv) Tumour size: 0 points for less than 5 cm, 2 points for more than 5 cm; (v) Nuclear grade: 0 points for grade 1 and 2, 1 point for grade 3, 2 points for grade 4; (vi) Necrosis: 0 points for no necrosis, 2 points for necrosis. The total score (0–15 points) was obtained by adding the 6 scores [11].

A follow-up physical examination, routine haematological index, and imaging such as CT or MRI were performed every 3–6 months 2 years after surgery and annually thereafter. The study endpoint was DFS, defined as the time between surgery and local recurrence or distant metastasis of kidney cancer or death from any cause. Survival was defined from the telephone interviews and the outpatient medical records. The follow-up period ended in December 2021.

### Statistical analysis

The patients were randomly divided into a training cohort and a validation cohort in a 7 : 3 ratio

until the 2 cohorts were not significantly different in terms of all the variables (*p*-value > 0.05, Table II).

The median and standard deviation of continuous variables were included in the descriptive analysis. The frequencies and proportions were analysed in the categorical variables. The *p*-value was computed by applying the rank sum test on continuous variables and the  $\chi^2$  test on categorical variables. The LASSO Cox regression (R software and “glmnet” package) was conducted to determine the DFS-related variables to develop predictive models for feature selection of high-dimensional variables and multicollinearity among variables. The optimal cut-off values of LMR were determined by using the X-tile software. The variables with *p* < 0.05 level were identified as statistically independent risk factors in the multivariate Cox regression analysis. The precision of the risk prediction model was assessed using the value of the Harrell’s C-index.

A 2-sided test was used for all the statistical tests. Statistically significant was defined as *p*-value < 0.05. The multivariate Cox regression analysis and the Harrell’s C-index were performed with R version 3.6.2. Moreover, the mean C-index was computed with Stata 14.0 (Stata Corp. Texas, USA).

## Results

### Baseline characteristics

In close compliance with the inclusion criteria, 612 patients with localized ccRCC who underwent

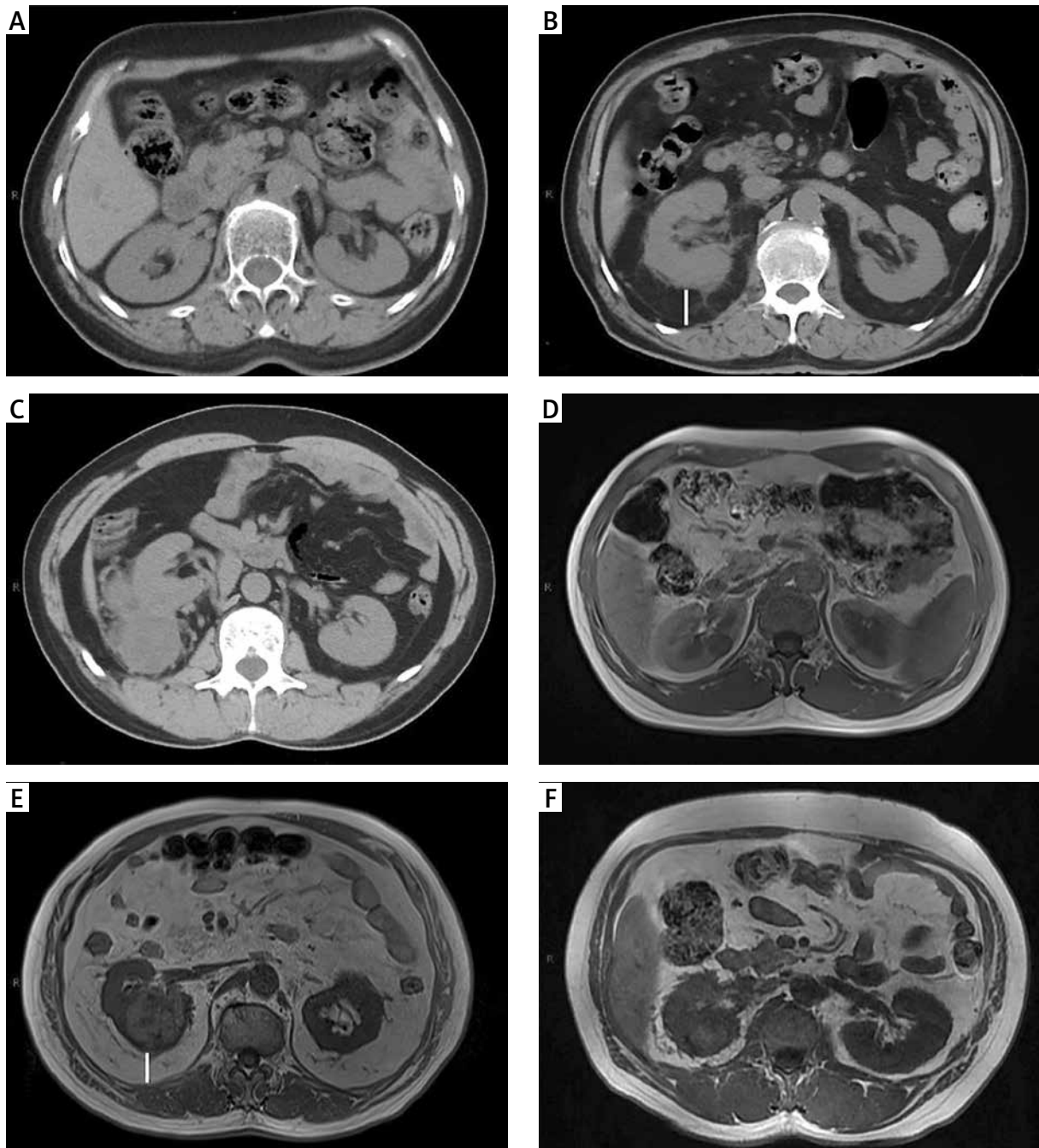


**Photo 1.** Mayo Adhesive Probability (MAP) score calculation—the thickness of the posterior renal fat (white line on the image) and grading of perinephric stranding on CT and MRI. **A, D** – No stranding: 0 points. The perirenal adipose tissue shows no stranding on **(A)** CT and **(D)** MRI. **B, E** – MAP score: 4 points. The thickness of the posterior renal fat is 2.4 cm (2 points) with moderate stranding (2 points) on **(B)** CT, and the posterior distance is 2.6 cm (2 points) with moderate stranding (2 points) on **(E)** MRI. **C, F** – Severe stranding: 3 points. The perirenal adipose tissue shows severe stranding with thick image-dense bars of inflammation on **(C)** CT and **(F)** MRI

*CT – computed tomography, MRI – magnetic resonance imaging.*

**Table II.** Baseline characteristics of the 612 patients

Variables	Overall (n = 612)	Training cohort (n = 414)	Validation cohort (n = 198)	P-value
Age [years]:				0.21
< 60	439 (71.7%)	290 (70.0%)	149 (75.3%)	
≥ 60	173 (28.3%)	124 (30.0%)	49 (24.7%)	
Sex:				0.31
Male	432 (70.6%)	298 (72.0%)	134 (67.7%)	
Female	180 (29.4%)	116 (28.0%)	64 (32.3%)	
Diabetes:				0.11
Yes	70 (11.4%)	41 (9.9%)	29 (14.6%)	
No	542 (88.6%)	373 (90.1%)	169 (85.4%)	
Hypertension:				0.60
Yes	180 (29.4%)	125 (30.2%)	55 (27.8%)	
No	432 (70.6%)	289 (69.8%)	143 (72.2%)	
Hyperlipidaemia:				0.45
Yes	4 (0.7%)	3 (0.7%)	1 (0.5%)	
No	608 (99.3%)	413 (99.3%)	197 (99.5%)	
CHD:				0.52
Yes	22 (3.6%)	13 (3.1%)	9 (4.5%)	
No	590 (96.4%)	401 (96.9%)	189 (95.5%)	
Smoking:				0.35
Yes	171 (27.9%)	121 (29.2%)	50 (25.3%)	
No	441 (72.1%)	293 (70.8%)	148 (74.7%)	
Drinking:				0.88
Yes	149 (24.3%)	102 (24.6%)	47 (23.7%)	
No	463 (75.7%)	312 (75.4%)	151 (76.3%)	
BMI [kg/m <sup>2</sup> ]				0.73
< 25	256 (41.8%)	170 (41.1%)	86 (43.4%)	
≥ 25	356 (58.2%)	244 (58.9%)	113 (56.6%)	
Laterality:				0.67
Left	281 (45.9%)	193 (46.6%)	88 (44.4%)	
Right	331 (54.1%)	221 (53.4%)	110 (55.6%)	
Operative type:				0.29
PN	220 (35.9%)	143 (34.5%)	77 (38.9%)	
RN	392 (64.1%)	271 (65.5%)	121 (61.1%)	
Nephrectomy:				0.23
Laparoscopic	193 (31.5%)	137 (33.1%)	56 (29.0%)	
Open	419 (68.5%)	277 (66.9%)	142 (71.0%)	
T stage:				0.57
T1	486 (79.4%)	324 (78.3%)	162 (81.8%)	
T2	17 (2.8%)	13 (3.1%)	4 (2.0%)	
T3	109 (17.8%)	77 (18.6%)	32 (16.2%)	

**Table II. Cont.**

Variables	Overall (n = 612)	Training cohort (n = 414)	Validation cohort (n = 198)	P-value
Fuhrman grade:				0.83
1	55 (9.0%)	36 (8.7%)	19 (9.6%)	
2	349 (57.0%)	228 (55.1%)	121 (61.1%)	
3	188 (30.7%)	131 (31.6%)	57 (28.8%)	
4	20 (3.3%)	19 (4.6%)	1 (0.5%)	
Necrosis:				0.66
Yes	57 (9.3%)	40 (9.7%)	17 (8.6%)	
No	555 (90.7%)	374 (90.3%)	181 (91.4%)	
Tumour size [cm]:				0.74
< 7	552 (90.2%)	374 (90.3%)	178 (89.9%)	
≥ 7	60 (9.8%)	40 (9.7%)	20 (10.1%)	
SSIGN:				0.17
0–3	544 (88.9%)	363 (87.7%)	181 (91.4%)	
4–7	62 (10.1%)	46 (11.1%)	16 (8.1%)	
8	6 (1.0%)	5 (1.2%)	1 (0.5%)	
MAPS:				0.66
0–3	511 (83.5%)	342 (82.6%)	169 (85.4%)	
4–5	101 (16.5%)	72 (17.4%)	29 (14.6%)	
CONUT score:				0.85
< 3	74 (12.1%)	52 (12.1%)	22 (11.1%)	
≥ 3	538 (87.9%)	362 (87.9%)	176 (88.9%)	
SIS score:				0.62
0	199 (32.5%)	133 (32.1%)	66 (33.3%)	
1	364 (59.5%)	249 (60.1%)	115 (58.1%)	
2	49 (8.0%)	32 (7.8%)	17 (8.6%)	
LMR				0.53
Mean ± SD	5.15 ±3.13	5.23 ±3.44	4.99 ±2.33	
Follow-up [months]				0.74
Mean ± SD	73.71 ±28.49	73.68 ±29.00	73.77 ±27.45	

CHD – coronary heart disease, BMI – body mass index, PN – partial nephrectomy, RN – radical nephrectomy, LMR – lymphocyte to monocyte ratio, SSIGN – the Mayo Clinic Stage, size, grade, and necrosis score, CONUT – controlling nutritional status score, MAPS – Mayo adhesive probability score, SIS – systemic inflammation score, SD – standard deviation.

surgery from January 2010 to December 2015 were incorporated and randomly divided into a training cohort (n = 414) and a validation cohort (n = 198) (Figure 1).

The study included 432 (70.6%) men and 180 (29.4%) women, with a mean age of 53.1 ±10.6 years. The pattern of age allocation was as follows: 173 (28.3%) patients ≥ 60 years and 439 (71.7%) patients < 60 years. A radical nephrectomy was con-

ducted in 392 (64.1%) patients and partial nephrectomy in 220 (35.9%) patients. The pathological stages T1, T2, and T3 were 486 (79.4%), 17 (2.8%), and 109 (17.8%) cases, respectively. Moreover, 55 (9.0%), 349 (57.0%), 188 (30.7%), and 20 (3.3%) cases were in Fuhrman grades 1, 2, 3, and 4, respectively. The mean follow-up period was 77.2 months. During the follow-up period, 92 (15.0%) patients had distant metastasis or local recurrence and 56 (9.2%) died, of

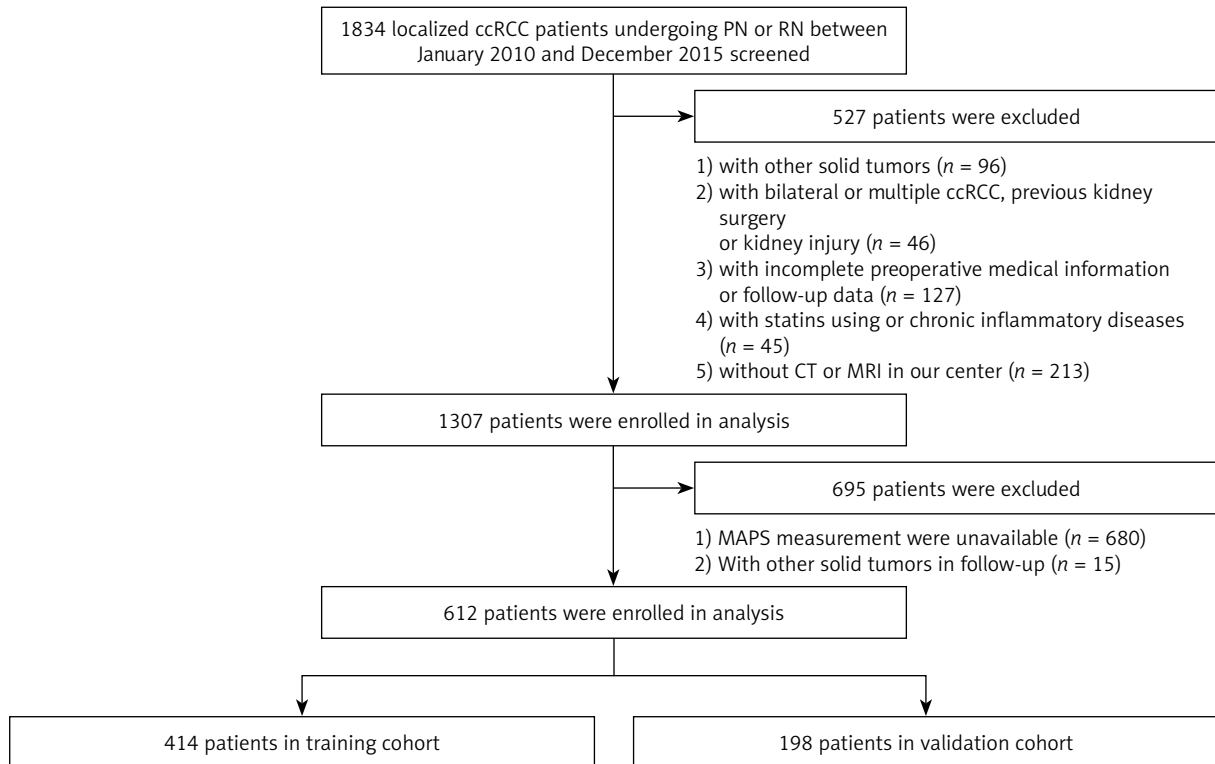


**Figure 1.** Patient selection flowchart

ccRCC – clear cell renal cell carcinoma, CT – computed tomography, PN – partial nephrectomy, RN – radical nephrectomy, MRI – magnetic resonance imaging, MAPS – Mayo adhesive probability score.

which 48 (7.8%) died of cancer. The 5-year DFS rate was 88.6% in the overall cohort.

**The prognosis values based on the LMR, SSIGN, and MAPS**

Among the 44 variables, the risk indicators (regression coefficients) selected by LASSO Cox regression were LMR (0.025) in blood indexes; Fuhrman tu-

mour grading, size, and SSIGN (0.062, 0.064, 0.222) on pathology; and MAPS (0.470) for images (Table III, Figures 2 A, B). The optimum cut-off value on the LMR was 2.80 (Figure 2 C), and the LMR ( $\geq 2.8$  vs.  $< 2.8$ ) was assigned points (0 or 1) to each indicator. According to the cut-offs in the literature, SSIGN (0–3 vs. 4–7 vs. 8) were assigned points (0, 1, 2), and MAPS (0–3 vs. 4–5) were assigned points (0 or 1)

**Table III.** Coefficients of significant variables screened by LASSO regression in the training cohort

Variables	Coefficients	HR
MAPS	0.470	1.601
SSIGN	0.222	1.249
Size	0.064	1.066
Fuhrman grade	0.062	1.063
LMR	0.025	1.025
Haemoglobin	-0.002	0.998
BMI	-0.021	0.979
Nephrectomy (laparoscopic/open surgery)	-0.157	0.854

BMI – body mass index, LMR – lymphocyte to monocyte ratio, HR – hazard ratio, SSIGN – the Mayo Clinic Stage – size – grade – and necrosis score, MAPS – Mayo adhesive probability score.

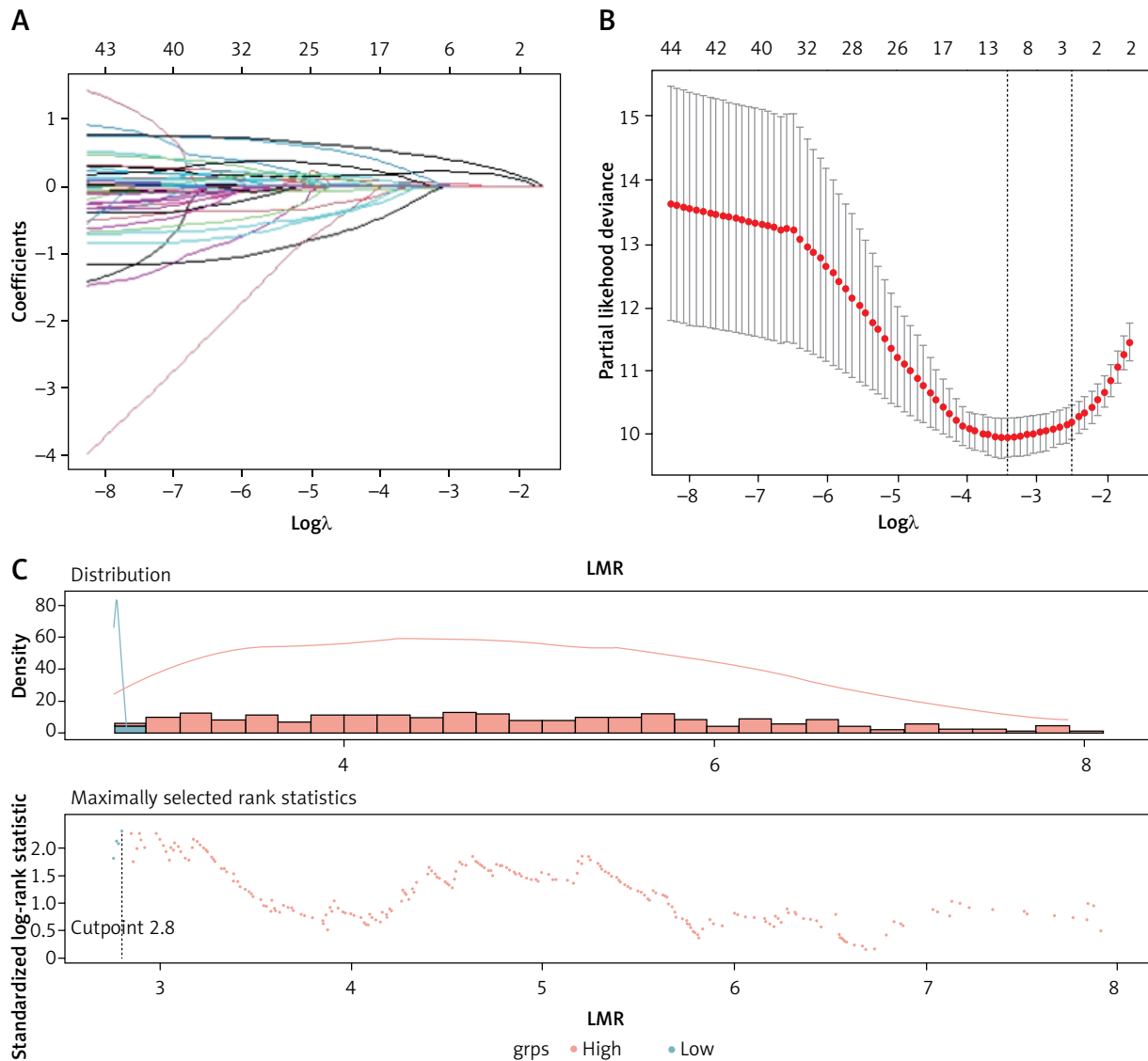
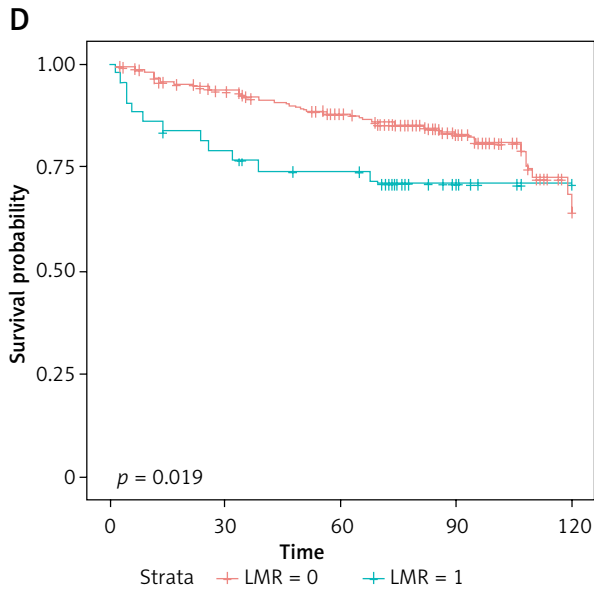


**Figure 2.** Clinical outcomes based on LMR, SSIGN, and MAPS. **A** – LASSO coefficient profiles of the 44 variables; **B** – 10-fold cross-validation for tuning parameter selection in the LASSO model; **C** – The optimal cut-off value for LMR

LMR – lymphocyte to monocyte ratio, SSIGN – the Mayo Clinic Stage, size, grade, and necrosis score, MAPS – Mayo adhesive probability score, DFS – disease-free survival.

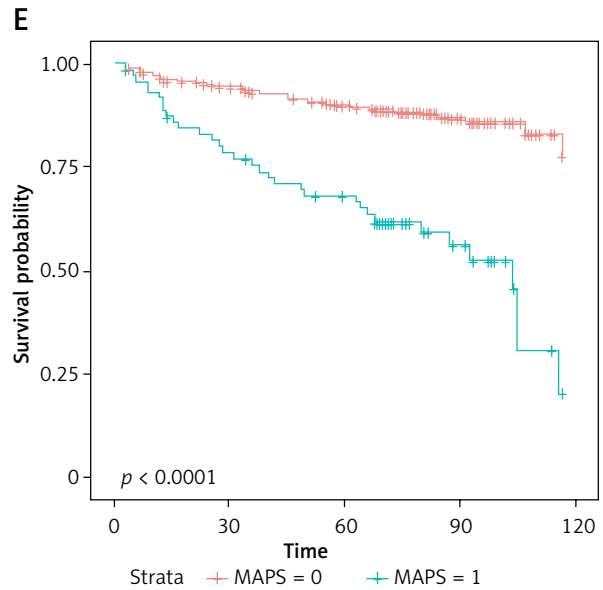




Number at risk

Strata	0	30	60	90	120
LMR = 0	371	331	297	116	17
LMR = 1	43	33	28	9	1

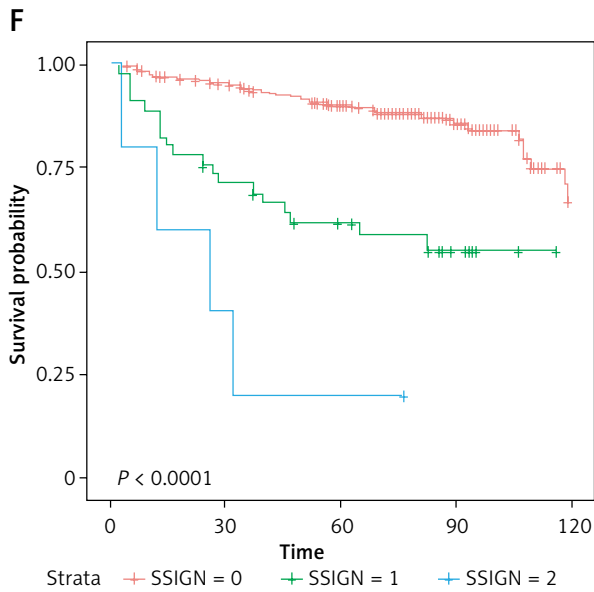
Time



Number at risk

Strata	0	30	60	90	120
MAPS = 0	342	310	280	106	16
MAPS = 1	72	54	45	19	2

Time



Number at risk

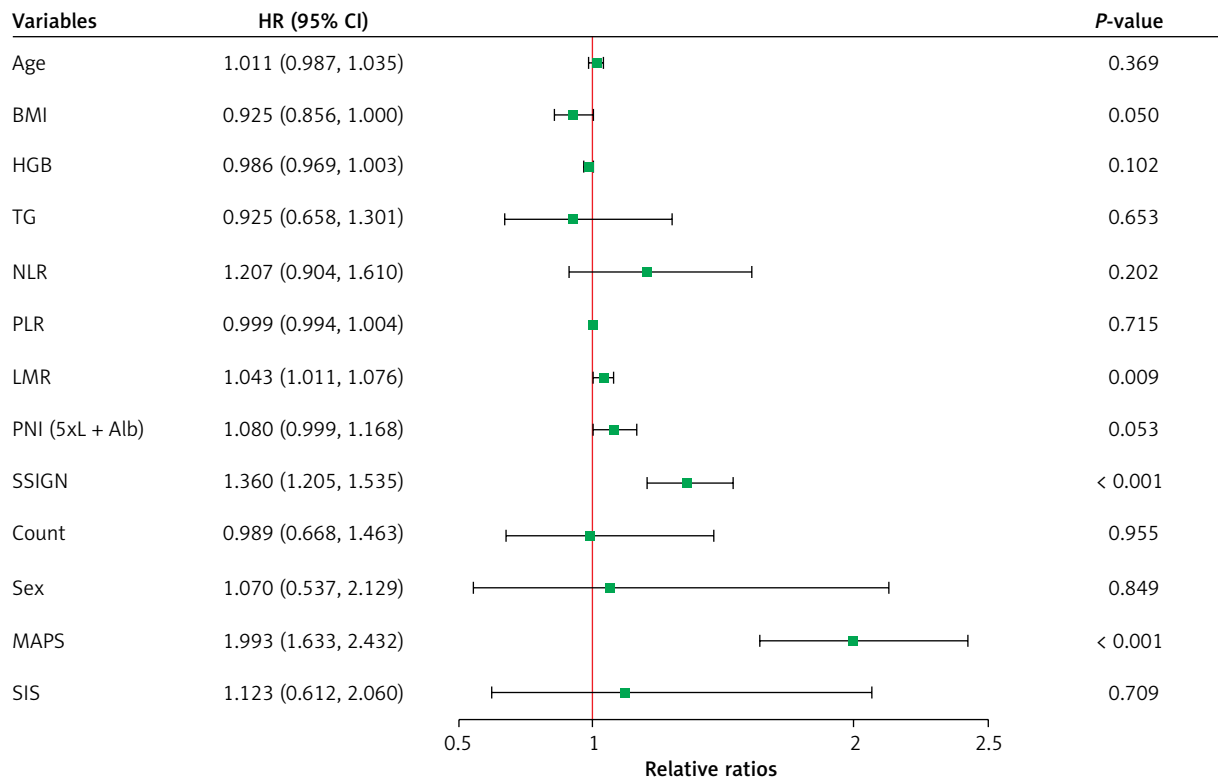
Strata	0	30	60	90	120
SSIGN = 0	363	331	300	118	18
SSIGN = 1	46	31	24	7	0
SSIGN = 2	5	2	1	0	0

Time

**Figure 2.** Cont. **D** – Kaplan-Meier analysis for DFS based on LMR. **E** – Kaplan-Meier analysis for DFS based on MAPS. **F** – Kaplan-Meier analysis for DFS based on SSIGN

LMR – lymphocyte to monocyte ratio, SSIGN – the Mayo Clinic Stage, size, grade, and necrosis score, MAPS – Mayo adhesive probability score, DFS – disease-free survival.

**A**



**B**

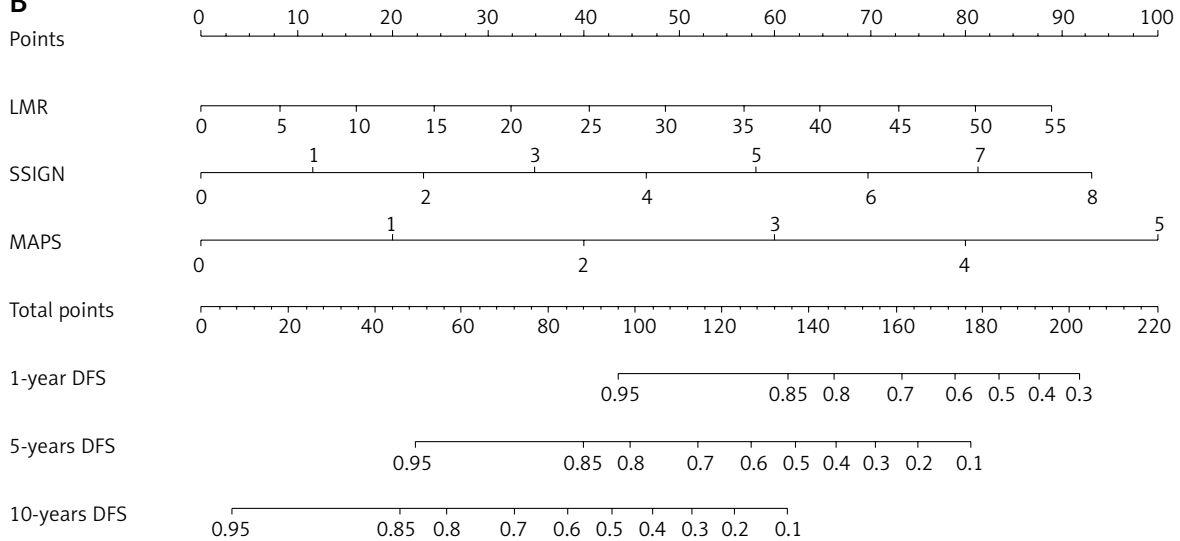


**Figure 3.** The construction of LMR-SSIGN-MAPS model. **A** – Multivariate Cox regression analysis in the training cohort. **B** – The LMR-SSIGN-MAPS model combining LMR, SSIGN, and MAPS

BMI – body mass index, TG – triglyceride, HGB – haemoglobin, NLR – neutrophil to lymphocyte ratio, PLR – platelet-to-lymphocyte ratio, LMR – lymphocyte to monocyte ratio, PNI – prognostic nutritional index, CONUT – controlling nutritional status score, SIS – systemic inflammation score, SSIGN – the Mayo Clinic Stage, size, grade, and necrosis score, MAPS – Mayo adhesive probability score.

to each indicator [10, 18]. The Kaplan-Meier survival analysis showed that LMR, MAPS, and SSIGN have significant prognosis values in predicting DFS ( $p = 0.019$ ,  $p < 0.0001$ , and  $p < 0.0001$ ) (Figures 2 D–F).

### Predictive risk LMR-SSIGN-MAPS model establishment

One multivariate Cox regression analysis of the training cohort further revealed that LMR (HR = 1.04,  $p = 0.009$ ), SSIGN (HR = 1.36,  $p < 0.001$ ), and MAPS (HR = 1.99,  $p < 0.001$ ) were considered to be independent risk variables (Figure 3 A). However, haemoglobin, body mass index (BMI), triglyceride, SIS, NLR, PLR, PNI, and CONUT were considered to be non-independent risk variables ( $p > 0.05$ ). Consequently, the LMR-SSIGN-MAPS (LSM) risk model combining LMR, SSIGN, and MAPS was constructed (Figure 3 B). The LMR-SSIGN-MAPS score was 0 in 434 (70.9%) cases, 1 in 258 (21.9%) cases, 2 in 32 (5.2%) cases, 3 in 10 (1.6%) cases, and 4 in 2 (0.3%) cases. Furthermore, patients were classified into low-risk (score 0), intermediate-risk (score 1 or 2), and high-risk (score 3 or 4) groups according to the LMR-SSIGN-MAPS model. The 5-year DFS rates were 94%, 77.1%, and 50%, respectively.

**Table IV.** Harrell's C-Index of prediction accuracy of LMR-SSIGN-MAPS and other models for DFS

Models	Training cohort (n = 414)	Validation cohort (n = 198)
	C-Index (95% CI)	C-Index (95% CI)
LMR-SSIGN-MAPS	0.854 (0.815–0.893)	0.848 (0.807–0.889)
SSIGN -MAPS	0.847 (0.806–0.888)	0.839 (0.805–0.891)
SSIGN	0.782 (0.777–0.787)	0.772 (0.699–0.845)

LMR – lymphocyte to monocyte ratio, SSIGN – the Mayo Clinic Stage, size, grade, and necrosis score, MAPS – Mayo adhesive probability score, C-index – Harrell's concordance index, DFS – disease-free survival, CI – confidence interval.

### Accuracy of the LMR-SSIGN-MAPS model compared with other models

The accuracy among the LMR-SSIGN-MAPS (model 1), SSIGN-MAPS (model 2), and SSIGN score (model 3) was compared using Harrell's C-index. The Harrell's C-index for LMR-SSIGN-MAPS were 0.854 (95% CI: 0.815–0.893) and 0.848 (95% CI: 0.807–0.889) comparing with SSIGN scores of 0.782 (95% CI: 0.777–0.787) and 0.772 (95% CI: 0.699–0.845) in the training and validation cohorts, respectively (Table IV, Figures 4 A, B). The Kaplan-Meier survival

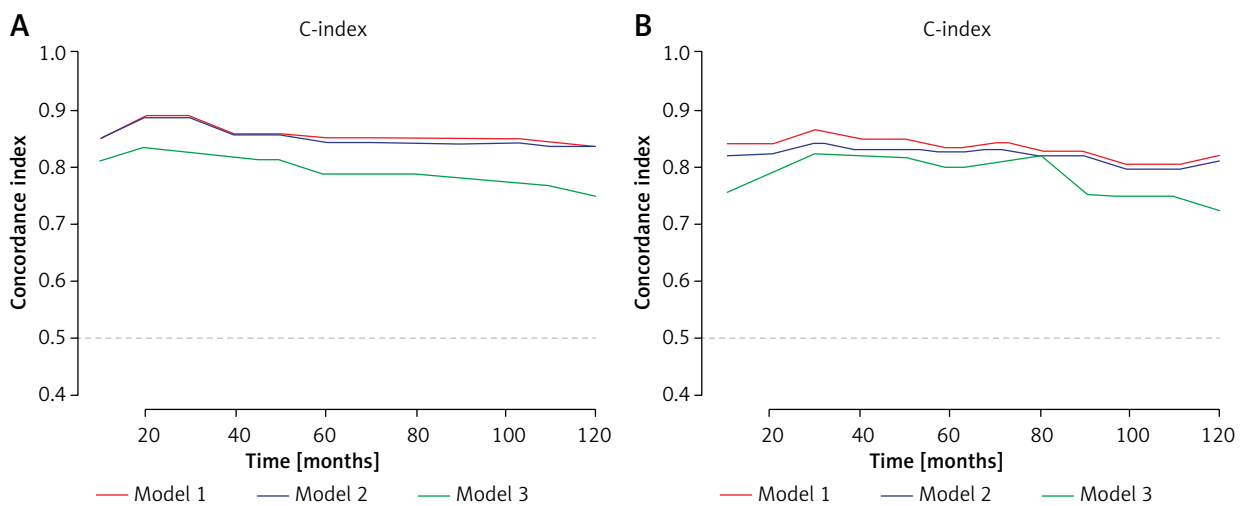


**Figure 4.** Accuracy of LMR-SSIGN-MAPS model compared with other models. **A** – Use the c-index to compare the LMR-SSIGN-MAPS model with the other models in the training cohort; **B** – Use the c-index to compare the LMR-SSIGN-MAPS model with the other models in the validation cohort. (model 1, LMR-SSIGN-MAPS score; model 2, SSIGN-MAPS score; model 3, SSIGN score)

DFS – disease-free survival, LMR – lymphocyte to monocyte ratio, C-index – Harrell's concordance (c)-index, SSIGN – the Mayo Clinic Stage, size, grade, and necrosis score, MAPS – Mayo adhesive probability score.

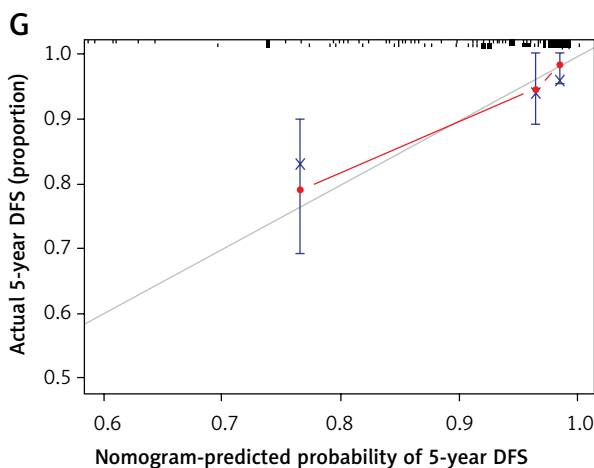
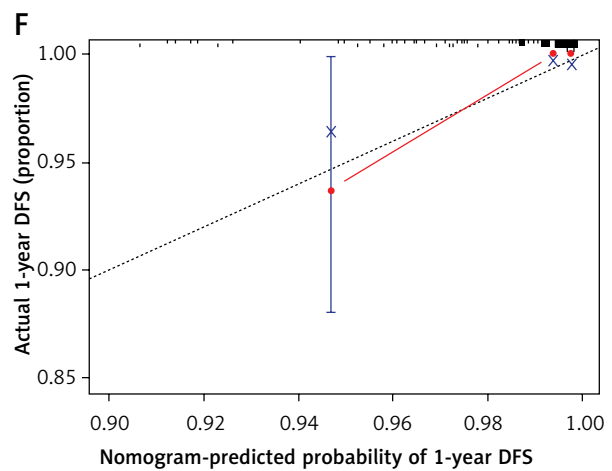
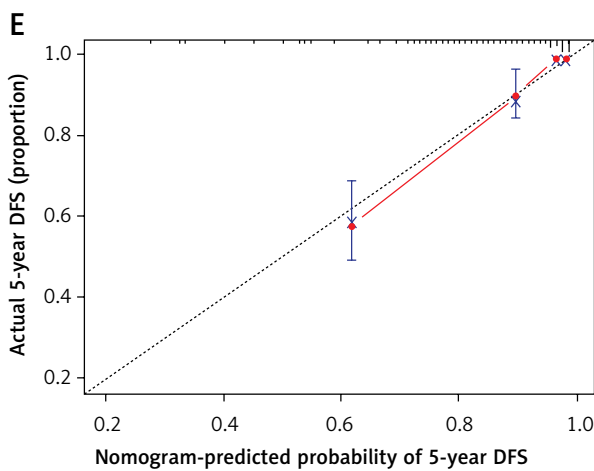
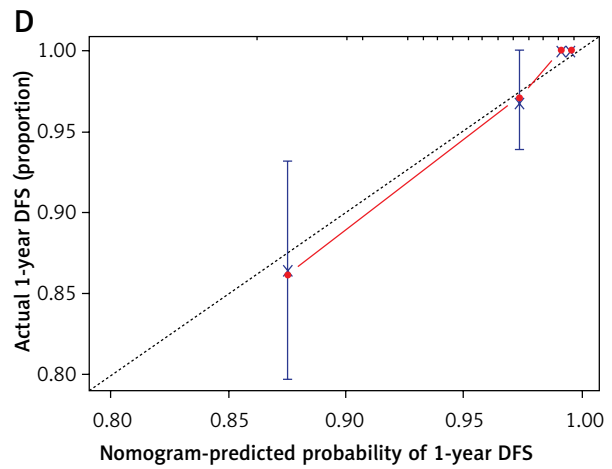
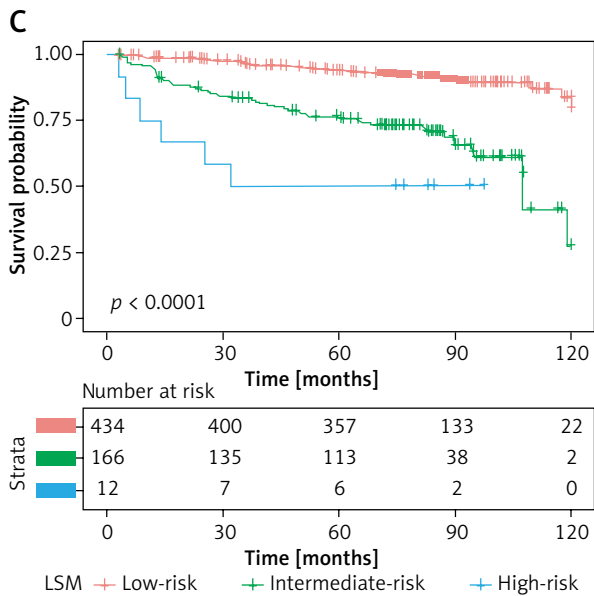


**Figure 4. Cont. C** – Kaplan-Meier analysis for DFS based on LMR-SSIGN-MAPS (LSM) model in the overall cohort. (low risk, LMR-SSIGN-MAPS score = 0; moderate risk, LMR-SSIGN-MAPS score = 1 or 2; high risk, LMR-SSIGN-MAPS score = 3 or 4); **D** – The calibration curve of the prediction for the patients' 1-year DFS in the training cohort; **E** – The calibration curve of the prediction for the patients' 5-year DFS in the training cohort; **F** – The calibration curve of the prediction for the patients' 1-year DFS in the validation cohort; **G** – The calibration curve of the prediction for the patients' 5-year DFS in the validation cohort

DFS – disease-free survival, LMR – lymphocyte to monocyte ratio, C-index – Harrell's concordance (c)-index, SSIGN – the Mayo Clinic Stage, size, grade, and necrosis score, MAPS – Mayo adhesive probability score.

analysis revealed that the stratified groups, based on the LMR-SSIGN-MAPS model, have significant differences in predicting DFS in localized ccRCC. Higher LMR-SSIGN-MAPS score was associated with poor DFS in the overall cohort ( $p < 0.0001$ ) (Figure 4 C). The calibration curves displayed that the predicted probabilities of 1.5-year DFS (Figures 4 D, E) in the training cohort and 1.5-year DFS (Figures 4 F, G) in the validation cohort matched well with the observed probabilities.

## Discussion

We constructed the predictive model of the integrated and developed LMR-SSIGN-MAPS score in patients with localized ccRCC. A higher LMR-SSIGN-MAPS score was significantly associated with poorer DFS. The finding identified that the LMR-SSIGN-MAPS, which consisted of preoperative biomarkers of inflammation, PRAT image-based scoring system, and pathology features demonstrated its strengths of simplicity and high predictive power.

Monocytes can differentiate into macrophages and dendritic cells. Furthermore, tumour-associated macrophages (TAMs) are the most dominant subpopulation of myeloid cells [19], which have been correlated with a poor prognosis [20]. Myeloid-derived suppressor cells (MDSCs) with tumour-promoting properties such as elimination of adapted antitumour immune responses and promotion of metastasis are a population of heterogeneous bone marrow cells [21]. The levels of monocytes can, at a certain level, represent the tumour burden of patients with cancer [5]. T cells are the predominant immune cell populations in the tumour microenvironment (TME) on ccRCC, with an average of 51% in the samples [22]. Comparatively low levels of lymphocytes may weaken tumour automonitoring and defence, leading to decreased antitumour efficacy [23]. Multiple studies have confirmed that LMR is a superior prognostic predictor for some tumours [5]. Therefore, patients with RCC with high LMR tend to experience advantageous urological outcomes. Our study proved that LMR was a significant independent risk variable ( $p = 0.009$ ), and a low level of LMR ( $< 2.80$ ) is associated with decreased DFS compared with high LMR ( $> 2.80$ ) in patients with localized ccRCC ( $p = 0.008$ ).

Because of the advantages of the videoscopic approach in terms of faster recovery, shorter hospi-

tal stay, and improved quality of life for the donor, Jakimowicz *et al.* showed that hand-assisted laparoscopic donor nephrectomy was a safe approach and should be used routinely instead of open surgery [24]. In our study, laparoscopic partial nephrectomy and laparoscopic radical nephrectomy also had the advantages of less surgical trauma, less bleeding, faster postoperative recovery, and fewer complications compared with open surgery, but the type of surgery was a non-independent risk variable (regression coefficients  $-0.157$ ). Furthermore, in spite of the Fuhrman grade and size were obtained by the LASSO Cox regression screening from 44 variables; (i) the SSIGN was constructed on the basis of clinic stage, size, grade, and necrosis which includes Fuhrman grade and size [11]; (ii) the regression coefficient of SSIGN was significantly higher than both Fuhrman grade and size; (iii) the SSIGN was reconfirmed as a significant risk variable by multivariate Cox regression analysis ( $p < 0.001$ ); and (iv) with 20 years of follow-up, the SSIGN continued to be a helpful prognostic tool, and the model kept its high predictive power for contemporary radical nephrectomy (RN) and partial nephrectomy (PN) patients [25]. Therefore, the SSIGN score was chosen for constructing a prognostic model, and high SSIGN scores were associated with decreased DFS in patients with localized ccRCC ( $p < 0.001$ ). However, SSIGN only included oncological features, and in our prediction model, SSIGN alone had a Harrell's C-index of 0.782, whereas in combination with LMR and MAPS, Harrell's C-index improved significantly to 0.854 in the training cohort.

Cancer cells can reprogram the metabolism of neighbouring noncancerous cells to provide extra energy substrates and metabolites for accelerated neoplasm growth [26]. Wei *et al.* reported that ccRCC cells produce a parathyroid hormone-related protein that facilitates PRAT browning through protein kinase A activation, leading to the release of excessive lactate to promote ccRCC growth, infiltration, and metastasis [8]. Adipose tissue secretes various adipokines, in particular vascular endothelial growth factor and interleukin 6, which are responsible for the induction of angiogenesis and inflammation, and they are correlated with a more invasive pathological profile and poor prognosis of RCC [27]. The MAPS is a score system calculated by measuring the thickness of the posterior renal fat (representing visceral obesity possibly) and the extent of perire-

nal fat stranding (representing organ inflammation possibly), which is correlated with progression-free survival in localized RCC [10]. Consistent with this report, our study proved that MAPS is a significant risk variable ( $p < 0.001$ ), and high MAPS was correlated with a decrease in DFS compared with lower MAPS in patients with localized ccRCC ( $p < 0.001$ ).

A growing body of predictive algorithms and nomograms were usually used for predicting the outcomes of RCC after surgery [28, 29]. In our study, the LMR-SSIGN-MAPS model was constructed for predicting DFS in patients with localized ccRCC. Because Harrell's C-index is more applicable to censored data [30], it is used to assess the model's predictive power. In training and validation cohorts, the LMR-SSIGN-MAPS model (Harrell's C-index, 0.854, 0.848) has higher accuracy compared with the SSIGN score (Harrell's C-index, 0.782, 0.772). Based on the LMR-SSIGN-MAPS model, the K-M survival analysis showed that higher LMR-SSIGN-MAPS scores were significantly correlated with poorer DFS in the overall cohort ( $p < 0.0001$ ). Therefore, the integrated prognostic model LMR-SSIGN-MAPS was in agreement with the view that multiple marker integration can be used to provide higher accuracy and predictive efficacy [31]. However, certain limitations with this model warrant further discussion. Firstly, the enrolment of patients exclusively from a single centre and the dependency of model formulation and verification on retrospective datasets predispose to a selection bias. Secondly, due to the slow update of the patients' image storage and retrieval system, fewer image data were available for early patients, and fewer figures were obtained as the time lengthened. Thirdly, the routine blood tests did not contain C-reactive protein before 2013 in our centre, so it was not possible to incorporate all potential correlates like C-reactive protein and the modified Glasgow prognostic score for LASSO Cox regression analysis. Finally, as Higuchi *et al.* pointed out, the real incident rate of abdominal wall pseudohernia is limited by the retrospective design of the study and the modest sample volume, and so it should be accurately quantified by more large-scale studies and further meta-analyses [32]. Because the validations were conducted internally, we were unable to rule out the possibility that the choice of variables and thresholds led to overfitting of the model, requiring external validations in further multicentre studies.

## Conclusions

The LMR-SSIGN-MAPS comprehensive prognostic model, consisting of preoperative inflammatory biomarkers, a PRAT image-based scoring system, and pathological features, showed the advantages of ease of use and high predictability and might be also used as a potential prognostic model for predicting DFS in patients with localized ccRCC.

## Acknowledgments

This study was partially supported by the National Natural Science Foundation of China (No. 81672555 and 81970216) and the Excellent Youth Science Foundation of Hebei Province (H2019206536). We thank the Yong Zhang team for precious resources and advice.

This retrospective study was approved by the Ethics Committee of the National Cancer Centre/Cancer Hospital, Chinese Academy of Medical Sciences and Peking Union Medical College (study number: 22/048-3249).

## Conflict of interest

The authors declare no conflict of interest.

## References

1. Sung H, Ferlay J, Siegel RL et al. Global Cancer Statistics 2020: GLOBOCAN Estimates of Incidence and Mortality Worldwide for 36 Cancers in 185 Countries. *CA Cancer J Clin* 2021; 71: 209-49.
2. Meskawi M, Sun M, Trinh QD, et al. A review of integrated staging systems for renal cell carcinoma. *Eur Urol* 2012; 62: 303-14.
3. Grivennikov SI, Greten FR, Karin M. Immunity, inflammation, and cancer. *Cell* 2010; 140: 883-99.
4. Nishida J, Momoi Y, Miyakuni K, et al. Epigenetic remodelling shapes inflammatory renal cancer and neutrophil-dependent metastasis. *Nat Cell Biol* 2020; 22: 465-75.
5. Chan JC, Chan DL, Diakos CI, et al. The lymphocyte-to-monocyte ratio is a superior predictor of overall survival in comparison to established biomarkers of resectable colorectal cancer. *Ann Surg* 2017; 265: 539-46.
6. Bedke J, Buse S, Pritsch M, et al. Perinephric and renal sinus fat infiltration in pT3a renal cell carcinoma: possible prognostic differences. *BJU Int* 2009; 103: 1349-54.
7. Shah PH, Lyon TD, Lohse CM, et al. Prognostic evaluation of perinephric fat, renal sinus fat, and renal vein invasion for patients with pathological stage T3a clear-cell renal cell carcinoma. *BJU Int* 2019; 123: 270-76.
8. Wei G, Sun H, Dong K, et al. The thermogenic activity of adjacent adipocytes fuels the progression of ccRCC and compro-

- mises anti-tumor therapeutic efficacy. *Cell Metab* 2021; 33: 2021-39.
9. Davidiuk AJ, Parker AS, Thomas CS, et al. Mayo adhesive probability score: an accurate image-based scoring system to predict adherent perinephric fat in partial nephrectomy. *Eur Urol* 2014; 66: 1165-71.
  10. Thiel DD, Davidiuk AJ, Meschia C, et al. Mayo adhesive probability score is associated with localized renal cell carcinoma progression-free survival. *Urology* 2016; 89: 54-60.
  11. Frank I, Blute ML, Cheville JC, et al. An outcome prediction model for patients with clear cell renal cell carcinoma treated with radical nephrectomy based on tumor stage, size, grade and necrosis: the SSIGN score. *J Urol* 2002; 168: 2395-400.
  12. Edge SB, Compton CC. The American Joint Committee on Cancer: the 7th edition of the AJCC cancer staging manual and the future of TNM. *Ann Surg Oncol* 2010; 17: 1471-4.
  13. Delahunt B, Sika-Paotonu D, Bethwaite PB, et al. Grading of clear cell renal cell carcinoma should be based on nucleolar prominence. *Am J Surg Pathol* 2011; 35: 1134-9.
  14. Castelli WP, Abbott RD, McNamara PM. Summary estimates of cholesterol used to predict coronary heart disease. *Circulation* 1983; 67: 730-4.
  15. Jeon HG, Choi DK, Sung HH, et al. Preoperative prognostic nutritional index is a significant predictor of survival in renal cell carcinoma patients undergoing nephrectomy. *Ann Surg Oncol* 2016; 23: 321-7.
  16. Ishihara H, Kondo T, Yoshida K, et al. Preoperative controlling nutritional status (CONUT) score as a novel predictive biomarker of survival in patients with localized urothelial carcinoma of the upper urinary tract treated with radical nephroureterectomy. *Urol Oncol* 2017; 35: 539 e9-39e16.
  17. Chang Y, An H, Xu L, et al. Systemic inflammation score predicts postoperative prognosis of patients with clear-cell renal cell carcinoma. *Br J Cancer* 2015; 113: 626-33.
  18. Ho TH, Kapur P, Eckel-Passow JE, et al. Multicenter Validation of enhancer of zeste homolog 2 expression as an independent prognostic marker in localized clear cell renal cell carcinoma. *J Clin Oncol* 2017; 35: 3706-13.
  19. Ginhoux F, Schultze JL, Murray PJ, et al. New insights into the multidimensional concept of macrophage ontogeny, activation and function. *Nat Immunol* 2016; 17: 34-40.
  20. Quail DF, Joyce JA. Microenvironmental regulation of tumor progression and metastasis. *Nat Med* 2013; 19: 1423-37.
  21. Gabrilovich DI, Ostrand-Rosenberg S, Bronte V. Coordinated regulation of myeloid cells by tumours. *Nat Rev Immunol* 2012; 12: 253-68.
  22. Chevrier S, Levine JH, Zanotelli VRT, et al. An immune atlas of clear cell renal cell carcinoma. *Cell* 2017; 169: 736-49.e18.
  23. Ferrone C, Dranoff G. Dual roles for immunity in gastrointestinal cancers. *J Clin Oncol* 2010; 28: 4045-51.
  24. Jakimowicz T, Macech M, Alsharabi A, et al. Hand-assisted laparoscopic donor nephrectomy: a single centre experience. *Videosurgery Miniinv* 2016; 11: 283-87.
  25. Parker WP, Cheville JC, Frank I, et al. Application of the stage, size, grade, and necrosis (SSIGN) score for clear cell renal cell carcinoma in contemporary patients. *Eur Urol* 2017; 71: 665-73.
  26. Fiaschi T, Marini A, Giannoni E, et al. Reciprocal metabolic reprogramming through lactate shuttle coordinately influences tumor-stroma interplay. *Cancer Res* 2012; 72: 5130-40.
  27. Park YH, Lee JK, Kim KM, et al. Visceral obesity in predicting oncologic outcomes of localized renal cell carcinoma. *J Urol* 2014; 192: 1043-9.
  28. Karakiewicz PI, Suardi N, Capitanio U, et al. A preoperative prognostic model for patients treated with nephrectomy for renal cell carcinoma. *Eur Urol* 2009; 55: 287-95.
  29. Yacyioglu O, Roberts WW, Chan T, et al. Prognostic assessment of nonmetastatic renal cell carcinoma: a clinically based model. *Urology* 2001; 58: 141-5.
  30. Kalderstam J, Edén P, Bendahl PO, et al. Training artificial neural networks directly on the concordance index for censored data using genetic algorithms. *Artif Intell Med* 2013; 58: 125-32.
  31. Guerrero C, Puig N, Cedena MT, et al. A machine learning model based on tumor and immune biomarkers to predict undetectable MRD and survival outcomes in multiple myeloma. *Clin Cancer Res* 2022; 28: 2598-609.
  32. Higuchi T, Shimizu K, Enoki K, et al. Risk factors for abdominal wall pseudohernia after percutaneous cryoablation of renal cell carcinoma. *Videosurgery Miniinv* 2022; 17: 188-93.

**Received:** 13.10.2022, **accepted:** 30.11.2022.